

CHAPTER 111

ESTIMATION USING A MOVABLE BED MODEL OF SHORELINE CHANGE CAUSED BY A RECLAMATION PROJECTED INTO THE SEA

by

Shoji SATO and Hiroaki OZASA
Port and Harbour Research Institute, Ministry of Transport,
1-1, 3-chome, Nagase, Yokosuka, Japan

INTRODUCTION

Recently, many local airports in Japan are considering to extend their runways, so accomodating passenger traffic. But most airports are obliged to extend their runways into the sea on account of the shortage of land and complaints from their neighbors about jet-plane noise. Tokushima Airport is one of such local airports, which is situated on the coast along the Kie-Suido Channel as shown Figure 1. The length of the runway of Tokushima Airport is 1500 m at present, so a plan to extend the runway by 600 m into the sea has been proposed by the local government. However, Matsushige beach, where the airport is located, is now so seriously eroded that offshore breakwaters are being constructed in the south and the northern part is used for sea-bathing. Therefore, it is necessary to estimate the change of beach profiles, especially of the shoreline, caused by the extension of the runway, and to find countermeasures against unfavourable change.

A movable bed model was constructed to estimate such changes, because no numerical simulation using a computer has been developed to estimate changes of a complicated beach topography. Of course, the universal dynamic similarity does not hold for model studies on sand transport problems. Therefore, the characteristics of sand transport at the site are first clarified through analysis of the field observation data, and then the model scale, bed material, and test waves are determined in such a manner that the topographic variation in the model sea bed will become similar to that in the prototype. But, in general, it is difficult to make all of the variations of the sea bed in the model similar to that in the prototype. In this model experiment, the long term changes of the shoreline has been taken as the most important phenomena to be reproduced in the model.

CHARACTERISTICS OF LITTORAL SEDIMENT TRANSPORT

The Matsushige coast, where the airport is located, is a sandy beach of 4000 m long bounded by the breakwaters of Imagiri and Awazu Ports. Waves from SSE-SE are overwhelmingly predominant, as seen in Table 1 which shows the deep water wave energy from each direction based on wave hindcasting using weather maps during the period from January 1971 to December 1975. Their wave heights, however, are usually less than 1.5 m as seen in Table 2, which shows waves of significant height more than one meter recorded on a wave recoder in 15 meters of water, from November 1975 to November 1976. Waves of more than 2 m high occur only when the typhoon passes near by the coast. Northerly waves occur

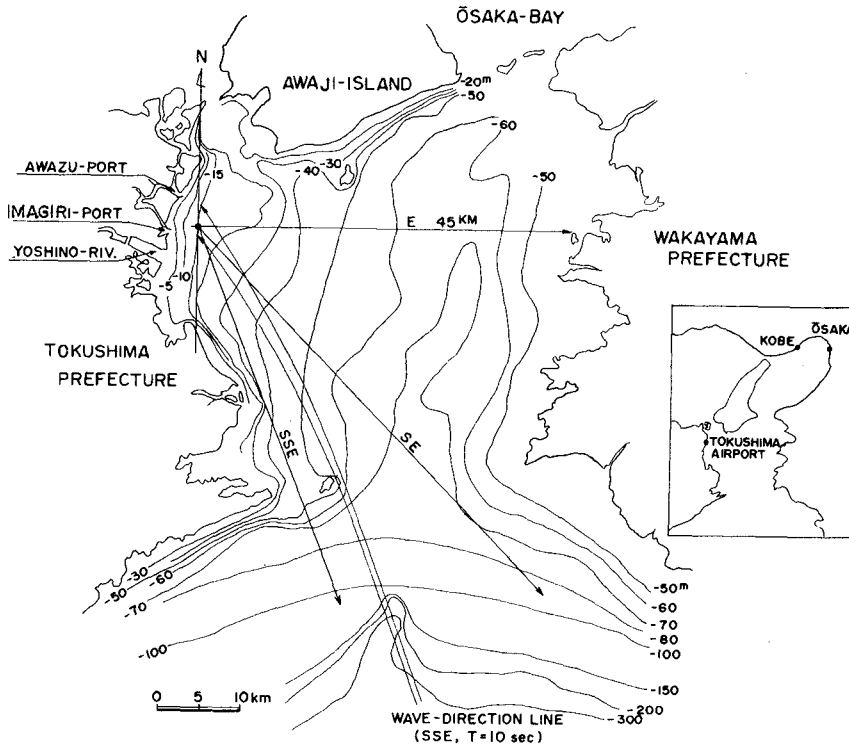


Figure 1. Situation of Tokushima Airport

DEEP WATER WAVE DIR.	WAVE ENERGY ($1 \cdot m/m$)
N E	1 2 0 2 0
E N E	3 4 0 0
E	5 3 0 0
E S E	1 2 5 4 0 0
S E	4 9 2 8 5 0
S S E	2 1 0 8 4 0 0
S	1 1 5 4 3 0

Table 1. Deep water wave energy based on wave hindcasting (Jan. 1971 to Dec. 1975)

DATE	$H_{1/3}$ (m)	$T_{1/3}$ (sec)
23 NOV. 1975	1.14	15.4
22 FEB. 1976	1.06	7.2
25 MAY 1976	1.31	15.1
24 JUL. 1976	1.42	10.8
13 SEP. 1976	1.31	7.0

Table 2. Observed waves of $H_{1/3}$ 1 m at the 15 m contour (nov. 1975 to Nov. 1976)

mostly in winter, but their height is usually less than one meter.

From the above wave characteristics, it is clear that the sand is predominantly transported along the coast from south to north. The Matsushige coast is located on the delta formed by the material discharged from the Yoshino River, the mouth of which is at about 2 km south of Imagiri Port. At present, however, littoral material transported into the coast from the south and transported out northward from the coast is very small in volume, on account of the construction of dams in the upstream areas of the Yoshino River and the completion of the breakwaters of Imagiri and Awazu Ports. So, the coast can be considered to be a nearly isolated beach from the standpoint of littoral sediment transport.

Figure 2 shows a contour map of the coast. At present, there is no sand beach within 1600 m from Imagiri Port, but from there it gradually appears, becoming 100 m wide at Awazu Port. Looking at the contours, 5 m line runs parallel to the coast from Awazu Port until the center of bay, and then turns seaward, and reaches the tip of the breakwater at Imagiri Port. Shallower contours tend to be parallel to the beach for a greater part of the bay, those less than 2 m being parallel all along it. Longshore bars occur only in the half of the bay near Awazu Port and are between 2 and 3 m deep. These contours also prove that the littoral transport is overwhelmingly northward in direction as mentioned above. The median diameter of the bed material is 0.3-0.36 mm on the beach, 0.2-0.24 mm on the bed at 5 m deep, and 0.1-0.13 mm on the bed at 10 m deep, as shown in Figure 2. A sea dike with crest height of 7 m above the datum level exists along all this stretch of the coast.

PRELIMINARY TEST

Method of The Preliminary Test

The waves for the main test which are able to cause littoral transport similar to that in the prototype clearly have SSE-direction in deep water, as seen in Table 1. Waves from SSE in deep water become SE in direction on 15 m contour owing to the refraction shown in Figure 1. Therefore, the bottom topography from the sea dike to the 15 m contour between Imagiri and Awazu Ports was produced in a wave basin with a scale of 1/200 horizontal and 1/50 vertical. The model area is shown in Figure 2. The part between 10 and 15 m contours was a fixed bed of concrete and the shallower part was made as a movable bed of sand with median diameter of 0.29 mm. The grain size distribution of the sand is shown in Figure 3.

This model test aim was to estimate long term changes of the bottom topography, especially of shoreline, caused by the extension of the runway. Past data on the long term changes of the bottom topography near the shoreline, therefore, are necessary in order to determine the wave condition for the main test. Unfortunately, no field surveys of the beach have not conducted in the past, except for a three years in recent, so that the past changes of the shoreline have been investigated using aerial photographs taken in different years. Figure 4 shows the shorelines in May 1964 and May 1969 which were found by that method.

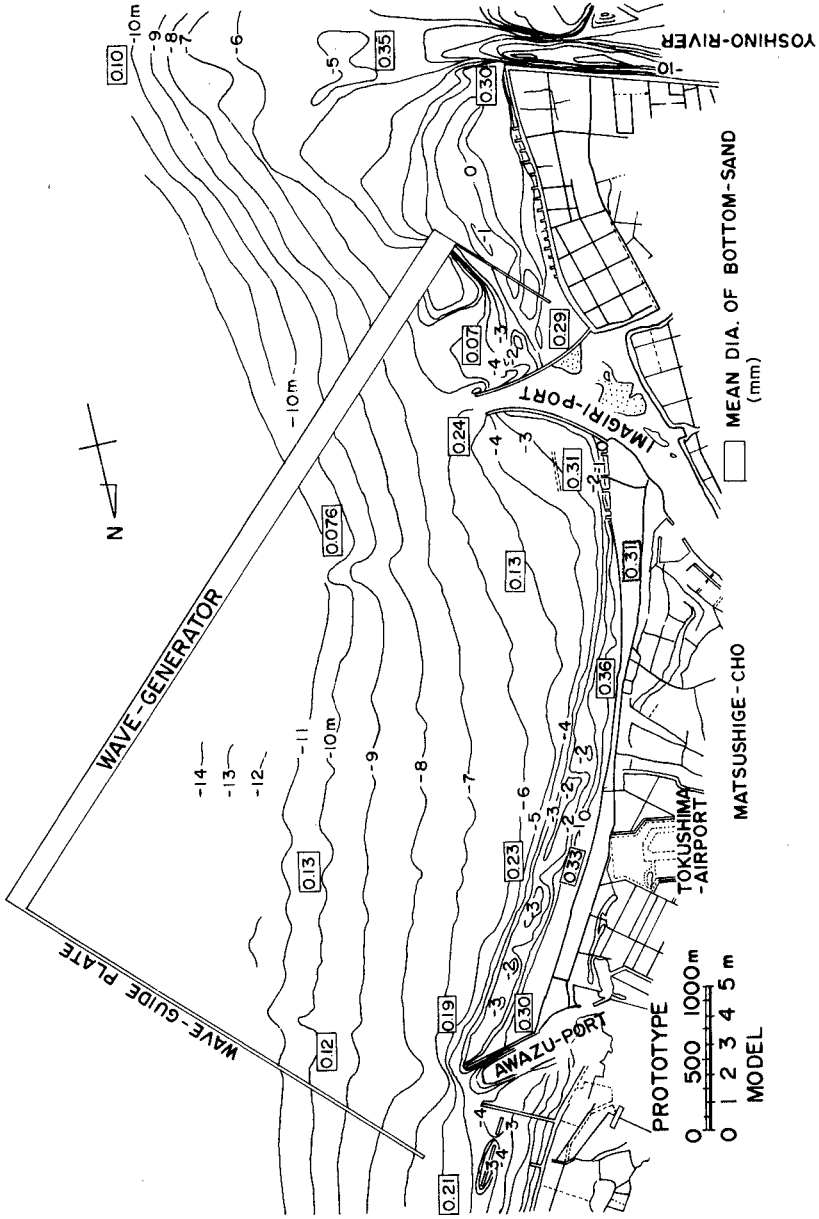


Figure 2. Contour map and the area of hydraulic model

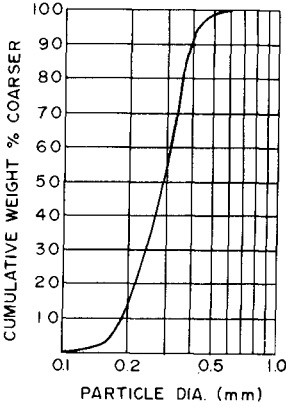
The breakwater of Imagiri Port had already been completed in May 1964, while the the south breakwater of Awazu Port was extend by 400 m, from 150 m long in May 1964 to 550 m long in May 1969. During those 5 years, the beach disappeared in the 1000 m nearest Imagiri Port and widen near Awazu Port.

The preliminary test was conducted by a trial and error method to find the most suitable SE-wave to produce the shoreline changes shown in Figure 4. Each wave, as shown in Table 3, was generated in the model where the bed topography was made to correspond to that of May 1964. The structures such as breakwaters were modeled to correspond to their state in May 1969. The bottom topography of May 1964 was obtained by the method shown in Figure 5, that is, the position of the shoreline investigated by using the aerial photograph of May 1964 was plotted with the beach profile of May 1975. Then the profile near the shoreline was drawn so that the same shape should be similar to that of May 1975. In order to check how the plan shape of the beach in the model approached that of the profile in May 1969 after wave action, the standard deviation of the former against the latter was calculated by the method shown in Figure 6. The position of the model was measured at 50 cm intervals (100 m in the prototype). The test was conducted at the level of M.W. which is one meter above the datum level. The scale of the wave period was taken as the square root of the vertical scale.

Result of The preliminary Test

Figure 7 shows changes of the above mentioned standard deviations during the experiment. The standard deviations, for all cases, decreased with the duration of the wave action, reaching a minimum value after some hours, then increasing. Among these cases, the standard deviation reached its smallest value for the case of waves of 5.3 cm in height and 1.13 sec period and its second smallest value for the case of the wave of 8.5 cm and 1.41 sec. Figure 8 shows the relation between H_o/L_o and H_o/d_{50} for each case, where H_o is the deep water wave height and d_{50} the median diameter of sand. The boundary lines between storm and normal beaches of Johnson (1949)¹⁾ and Iwagaki-Noda (1963)²⁾ are also shown in the figure. Comparing the test data with these boundary lines, it is found that Cases 1 and 5 which have the smaller minimum values of standard deviation are nearly on the boundary lines, but Cases 2 and 6, having larger values are a long way from them. Figure 9 shows the shorelines for each case at the time when it approached nearest the position of the prototype in May 1969. Cases 1 and 5 coincide with the shoreline of May 1969 fairly well, but Cases 2 and 6 deviate respectively seawards and landwards. The waves of Cases 2 and 6 are considered to be respectively accumulative and erosive waves.

In order to determine the wave condition for the main test, it is also necessary to the quantity of sand movement in the offshore zone as well as the comparison of the shorelines as mentioned above. In Case 5, which has waves of 5.3 cm in height and 1.13 sec period, sand ripples were not seen in some areas of the offshore zone deeper than about 16 cm (8 m in the prototype). On the other hand, in Case 1, which has waves of 8.5 cm in height and 1.41 sec period, they were seen in all area of



CASE	MODEL		PROTOTYPE	
	H (cm)	T (Sec)	H (m)	T (Sec)
1	8.5	1.41	4.3	10
2	6.2	1.71	3.1	12
3	5.8	1.41	2.9	10
4	6.8	1.41	3.4	10
5	5.3	1.13	2.7	8
6	7.4	1.13	3.7	8

Table 3. Dimension of the waves in the preliminary test

Figure 3. Grain size distribution of the sand used as movable material

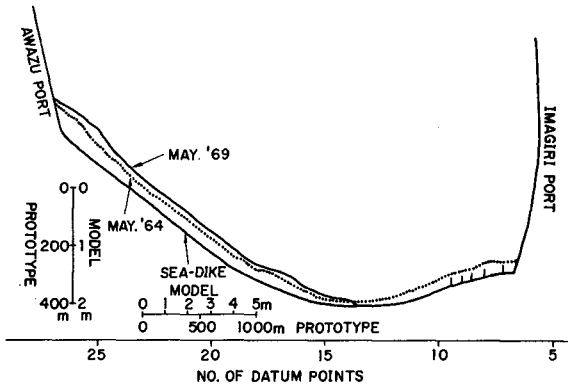


Figure 4. Shorelines of 1964 and 1969 found by using aerial photographs

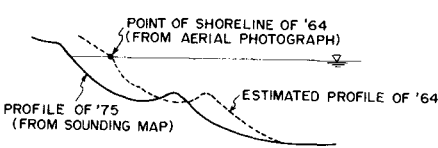


Figure 5. Method of estimating the bed topography of May 1964

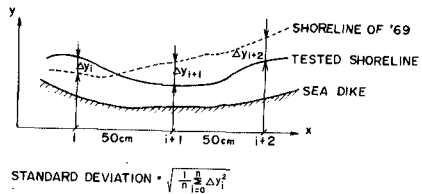


Figure 6. Calculation of the standard deviation of the shoreline

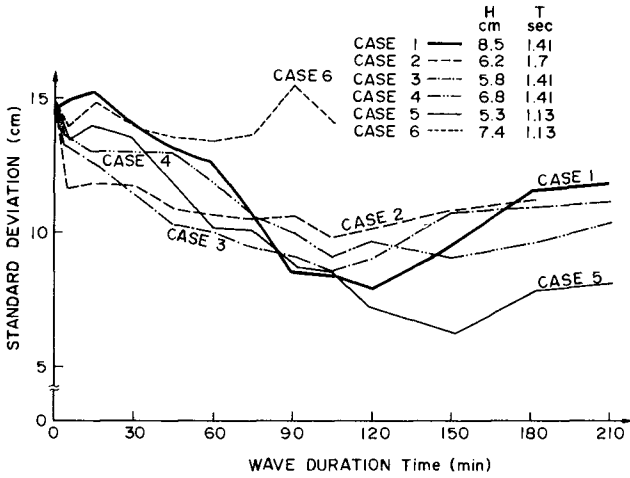


Figure 7. Changes of the standard deviations of the shorelines due to the wave action

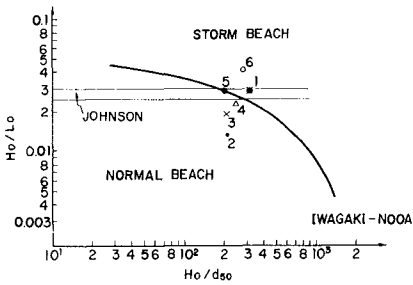


Figure 8. Relation between model waves and the boundary lines between storm and normal beach

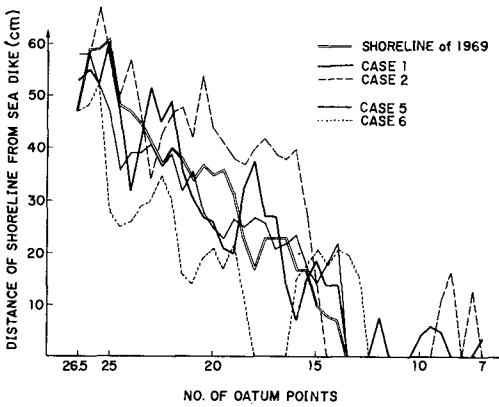


Figure 9. Comparison of the model shorelines when they approached nearest the actual shoreline of May 1969

the movable bed.

The critical water depth h , where all sand particles of the surface layer of the sand bottom are moved collectively in the direction of the wave propagation on the open sea without strong currents, is expressed by Sato-Ijima-Tanaka (1962)³ as follows:

$$\frac{H_o}{L_o} = 1.35 \left(\frac{d}{L_o}\right)^{1/3} \left(\sinh \frac{2\pi h}{L}\right) \left(\frac{H_o}{H}\right) \quad (1)$$

Where H_o and L_o are the height and the length of deep water waves, H and L are the height and the length of the waves at the critical water depth h , and d the diameter of bottom sand. The calculation diagram of Equation (1) is shown in Appendix. The length of the deep water wave of $T = 1.41$ sec is

$$L_o = 1.56 \times (1.41)^2 = 3.10 \text{ m}$$

Using small amplitude wave theory, the dimension of the deep water wave for $H = 8.5$ cm and $T = 1.41$ sec at 30 cm deep is obtained to be $H_o = 9.13$ cm. Using $d = 0.29$ mm in the model,

$$\frac{H_o}{L_o} = \frac{0.0913}{3.10} = 0.0295, \quad \frac{d}{L_o} = \frac{0.29 \times 10^{-3}}{3.10} = 9.35 \times 10^{-5}$$

According to Figure (A-3) in Appendix, $h/L_o = 0.038$. So,

$$h = 0.038 \times 310 = 11.8 \text{ cm}$$

The critical water depth $h = 11.8$ cm corresponds to $h = 5.9$ cm in the prototype. The critical wave height H_o for $T = 10$ sec, $h = 5.9$ m, and $d = 0.23$ mm in the prototype is calculated as follows:

$$\frac{d}{L_o} = \frac{0.23 \times 10^{-3}}{156} = 1.47 \times 10^{-6}, \quad \frac{h}{L_o} = \frac{5.9}{156} = 0.038$$

By the same figure in Appendix, $H_o/L_o = 0.0075$ is given. So,

$$H_o = 0.075 \times 156 = 1.2 \text{ m}$$

That is, the waves of Case 1 nearly correspond to a significant wave of $H_o = 1.2$ m and $T = 10$ sec in the prototype from the standpoint of the sand movement in the offshore zone. Also, it is found that the critical water depth for Case 5 is 6 cm and that the waves of Case 5 nearly correspond to a significant wave height of $H_o = 0.7$ m and period of $T = 10$ sec in the prototype from the same standpoint.

On the other hand, according to the observation data shown in Table 2, the wave height in the normal storm would be expected to be 1.0–1.5 m. Therefore, the wave for the main test was determined to be the wave from SE of 8.5 cm height and 1.41 sec period. This wave reproduced the shoreline change from 1964 to 1969 after 120 minutes of the run, as shown in Figure 7; the time scale for the shoreline changes would be approximately 120 minutes in the model to 5 years in the prototype.

MAIN TEST

Test Cases

The determined wave condition was generated for 6 hours on each of the following four cases:

- Case 1: The present bottom configuration which was surveyed in 1975
- Case 2: Reclamation for the runway extension is added to Case 1
- Case 3: A single line of offshore breakwaters along the coast south of the runway reclamation and a long offshore breakwater along the north coast are added to Case 2

Case 4: Double lines of offshore breakwaters along the southern part of the coast and three short offshore breakwaters along the northern part are added to Case 2

The models of offshore breakwaters are rectangular boxes of wire netting filled by small gravel, so they are permeable. The crest height is 8 cm (4 m in prototype) above the datum level, though that of the prototype actually is 2.5 m. This is because the model wave height is larger than 1/50 of the prototype wave height for a normal storm as mentioned before. Where the beach was eroded so severely that waves struck directly on the sea dike, same gravel was placed in front of it. The sea wall around the runway reclamation was faced by wave absorbers of gravel. The water level was set at the mean water level, the same as that in the preliminary test.

Changes of The Shoreline

The lines of the mean water level are shown in Figure 10 for before the wave action and after 360 minutes of it. Not that longitudinal and lateral scales are different. Using the time scale obtained in the preliminary test, 360 minutes of wave action nearly corresponds to 15 years in the prototype. The following changes of the shoreline can be deduced from the figure.

(1) The coast between the runway reclamation and Imagiri Port
From the result of Case 1, it can be seen that the coast will carry on eroding if it remains in the present state without any countermeasures; the beach above M.W.L. would disappear moreover over a stretch of about one kilometer after 15 years. But, if the runway reclamation is carried, the coastal erosion would be cease in some areas; the loss of the beach above M.W.L. after 15 years only occurs over half the stretch affected in Case 1. Moreover, if the offshore breakwaters are added as in Case 3, the distance over which the beach would disappear reduces to 300 m. In Case 4 with the double lines of offshore breakwaters set in zigzag-pattern, the beach would be formed to the south of the present one.

(2) The coast between the runway reclamation and Awazu Port
From the result of Case 1, the beach is clearly going to continue accreting if it remains in the present state. On the other hand, if the runway reclamation is constructed, the width of the beach would increase near the breakwater of Awazu Port and the reclamation, and decrease a little between them. As a result, the shape of the beach line would become concave. Though such a concave shoreline was not considered to be inconvenient for sea-bathing, measures to keep the shoreline straight were researched in Cases 3 and 4. In Case 3 with a long offshore breakwater, the beach erodes near Awazu Port and accumulates elsewhere. In Case 4 with three short offshore breakwaters, the beach accumulates throughout, keeping an almost straight shoreline. The distance between the offshore breakwaters and the shoreline, however, becomes so small as to be inconvenient for sea-bathing.

Changes of The bottom Topography

Figure 11 shows the contours for Case 1. (a) in the figure, which

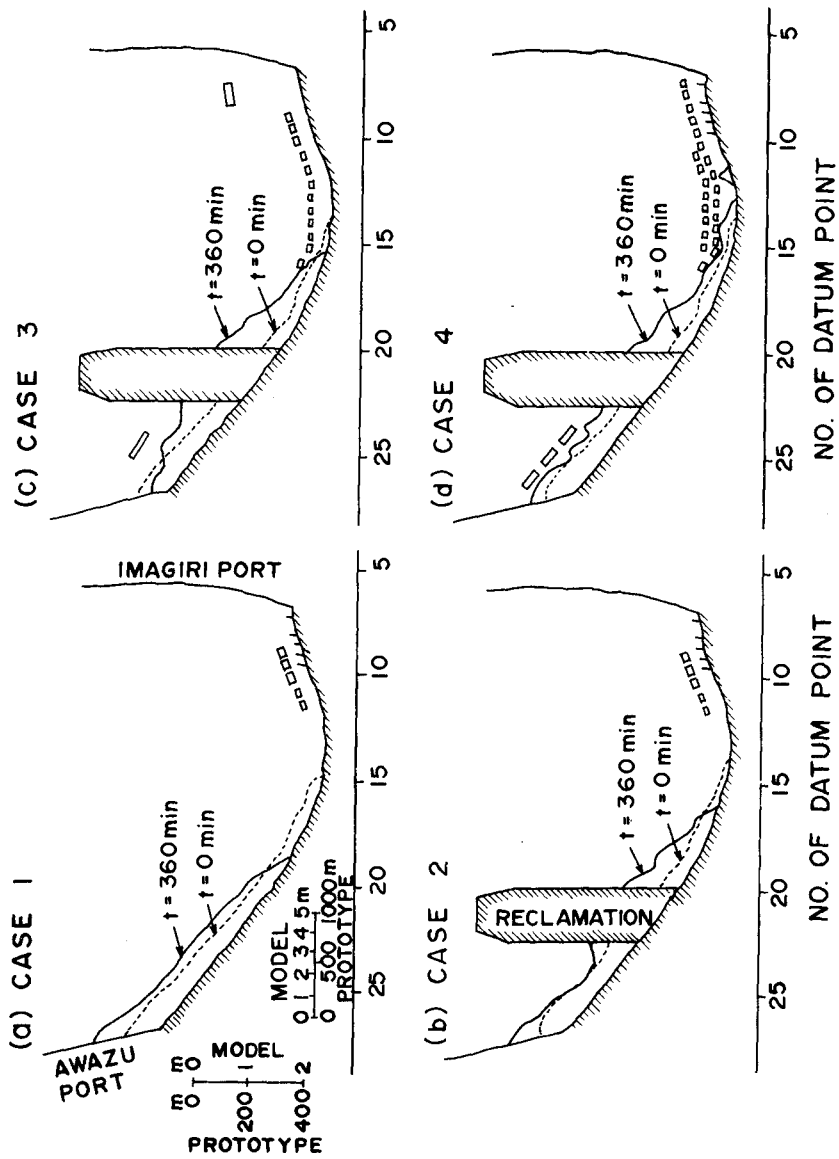


Figure 10. Changes of the lines of m.w.l.

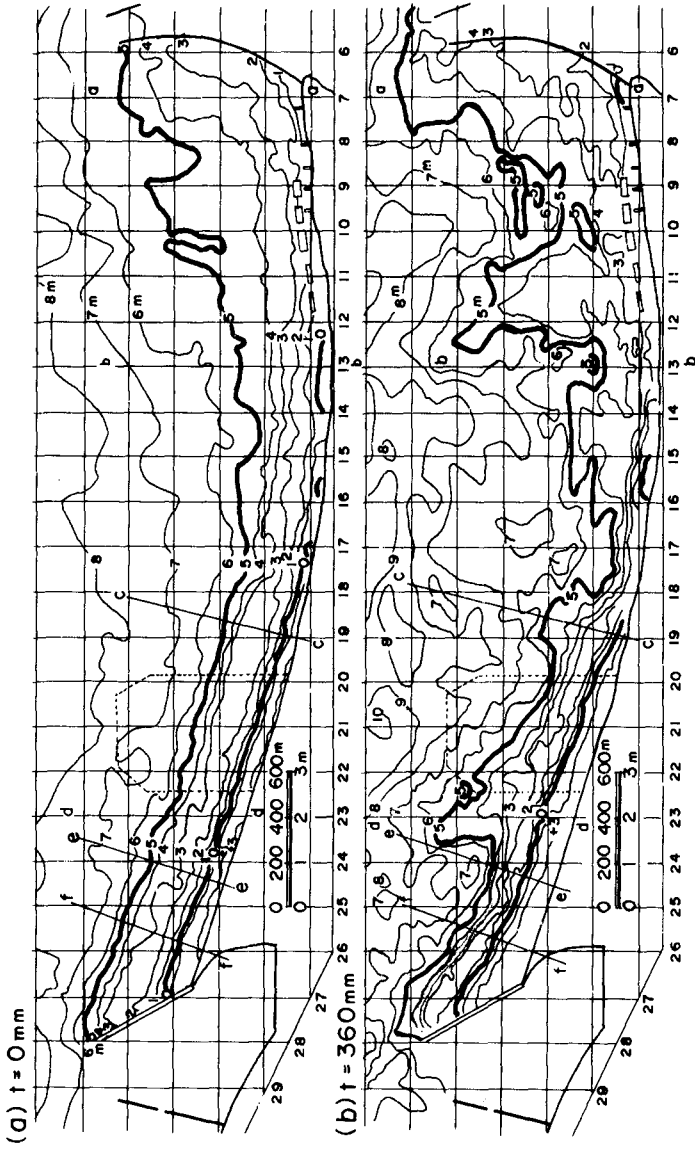


Figure 11. Changes of the bottom topography

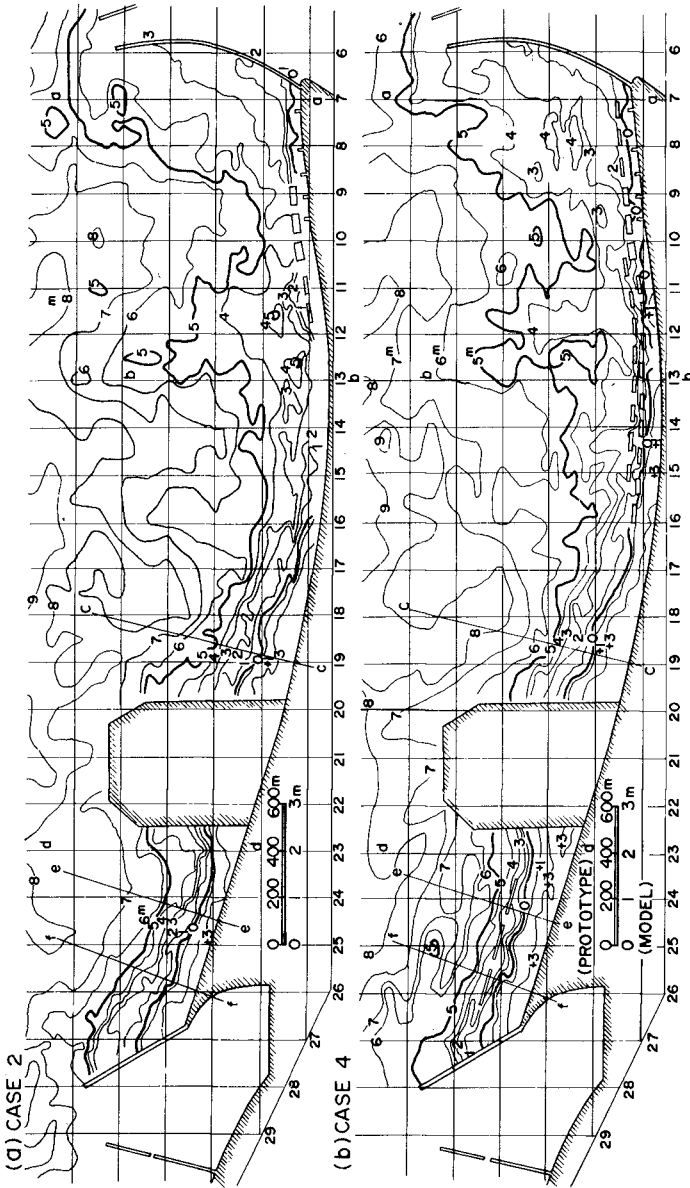


Figure 12. Contours after 360 minutes of wave action for Cases 2 and 4

is before wave action, is the bottom topography of 1975. The beach above 0 m is not exposed over a stretch of 1100 m near the south end of the bay and has a width of 100 m at the north end. In the contour map after 360 minutes of the run shown in (b) of the figure, the 5 m contour recedes landwards considerably in the areas near datum points Nos. 9-10 and 13 at the south end and Nos. 16-18 in the central part. It advances seawards considerably at the area of points Nos. 11-12 and 22-23. The contour of 5 m also advances seawards in the vicinity of the tips of the breakwaters of Imagiri and Awazu Ports. In the area near the shoreline, there is clearly a tendency of erosion in the south and of accumulation in the north; the beach above 0 m is not exposed for a stretch of 2200 m near Imagiri Port but increases to 200 m in width in the vicinity of Awazu Port.

Figure 12 shows the contours after 360 minutes of the run for Cases 2 and 4. Needless to say, the contours before the run for the both cases are the same as (a) in Figure 11. The followings can be deduced from (a) of Figure 12 in comparison with (a) of Figure 11:

(1) The 5 m contour recedes landwards in the area of Nos. 9-10 and advances seawards in the area of Nos. 11-12 as remarkably as in Case 1 but does not recede in the areas of Nos. 13 and 16-18. It, in fact, advances seaward in the vicinity of the runway extension.

(2) In the vicinity of the shoreline, a wide beach appears just at the south side of the runway reclamation, and the width of the beach between the reclamation and the south breakwater of Awazu Port becomes a littil narrower than in Case 1.

(3) The 5 m contour recedes landwards a littil at the tip of the south breakwater of Awazu Port, which is different from Case 1.

Comparing (a) and (b) in Figure 12, the points of difference points between Cases 2 and 4 are as follows:

(1) In the area between the runway reclamation and Imagiri Port, a beach above 0 m appears in front of the sea dike almost along its length in Case 4 and the contours between 1 and 5 m recede a littil further landwards in Case 4 than in Case 2.

(2) In the area between the runway reclamation and Awazu Port, the line of 0 m advances further seawards in Case 4 than in Case 2, though it runs in a rather straighter line.

Figure 13 shows the changes of the beach ploffiles after 360 minutes of wave action for Cases 1, 2, and 4. The profiles shown in the figure are along the lines a-a, b-b, c-c, d-d, e-e, and f-f of Figure 11 and 12. The profile a-a, which is near Imagiri Port, accumulates most in Case 1. The profile b-b, which is about 1300 m from the north breakwater of Imagiri Port, erodes in Cases 1 and 2, but accumulates at the shoreline of Case 4. The profile c-c accumulates in all cases, but more so in Cases 2 and 4 as a result of the runway extension. The profiles d-d, e-e, and f-f accumulate more in Case 1 than in Cases 2 and 4, and, comparing Cases 2 and 4, the area in the vicinity of the shoreline accumulates more in Case 4 than in Case 2.

The Rate of Littoral Sediment Transport

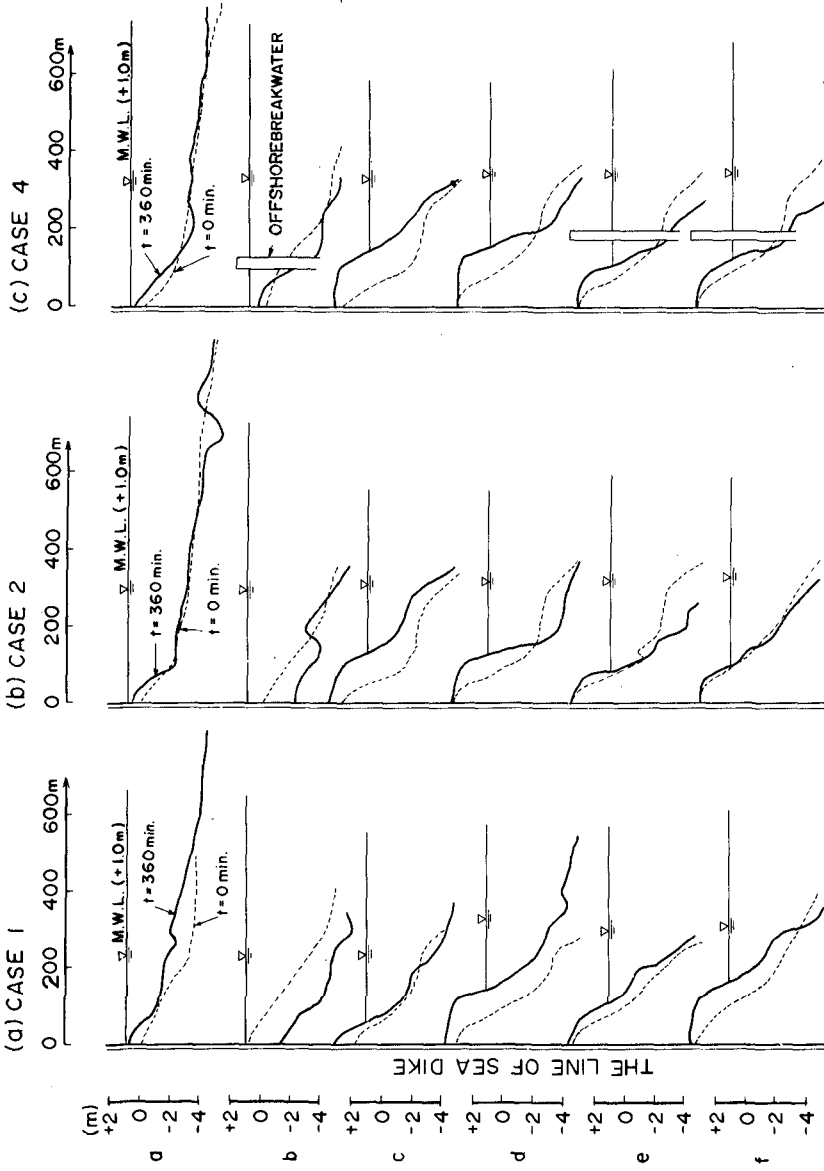


Figure 13. Changes of the beach profiles

The littoral sediment transport was measured in Cases 1 and 2 by using sand traps. A unit of the sand traps is a stainless steel box of 10 cm high and 30 cm wide, and has wings of 15 cm long on both sides, as shown in Figure 14. In Case 1, from minutes 120 to 130 of the run, the sand traps were set from the sea dike to the 7 m contour, in perpendicular to the shoreline on the line passing datum point No. 20 which lies on the proposed runway reclamation. In Case 2, from minutes 200 to 210 of the run, they were set seawards from the 7 meters contour on the same line as Case 1. These results are shown in Figure 15, where the volume of sand trapped in each trap is shown by dry weight. Most littoral transport is found to be concentrated landwards of the longshore bars as in the prototype. The peak values of trapped sand at the seaward end, in Cases 1 and 2, are considered to be caused by sand entering the trap from its offshore edge. On the other hand, the peak value at the landward end in Case 2 is thought to be due to sand travelling along the sea wall of the runway reclamation from the south.

From the results mentioned above, the total littoral transport rate in the case without the runway reclamation can be deduced to be the sum of the following two volumes:

11800 g/10 minutes minus the peak value of the seaward end (in Case 1)

and

2200 g/10 minutes minus the peak value of the landward end (in Case 2)

This gives 1200 g/minute. In the case with the runway reclamation, the transport is 2200 g/10 minutes from Case 2, that is, 220 g/minute.

The apparent specific gravity of sand in the sea bottom is supposed to be 1.6. 24 minutes in the model corresponds to one year in the prototype on the basis of the preliminary test. Considering, moreover, that the volume ratio of the prototype against the model is $200^2 \times 50$, the littoral sediment transport rate in the prototype would be calculated as follows:

(1) For the case without the runway reclamation

$$1200 \times \frac{1}{1.6} \times 24 \times 200^2 \times 50 \times 10^{-6} \doteq 36000 \text{ m}^3/\text{year}$$

(2) The littoral transport rate passing the offshore side of the runway reclamation

$$2200 \times \frac{1}{1.6} \times 24 \times 200^2 \times 50 \times 10^{-6} \doteq 6600 \text{ m}^3/\text{year}$$

On the other hand, the longshore wave energy which was calculated by using weather maps in period from 1971 to 1976 is shown in Table 4. The net longshore wave energy flux per year, according to Table 4, is approximately 1.9×10^5 ton·m/m northward. The relation between the littoral transport rate Q_i and the longshore wave energy flux E_i , on the basis of the diagram of Savage (1964)⁴, is given as follows:

$$Q_i = 0.21 E_i$$

Where Q_i is in unit of cubic meters and E_i ton·m/m. Substituting the value of 1.9×10^5 mentioned above for E_i in this equation, the littoral

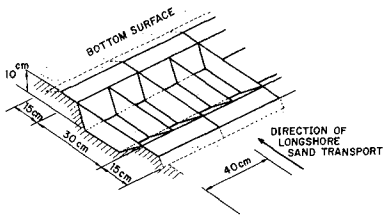


Figure 14. Sketch of the sand traps

Direction of Deep-water wave	Longshore Energy Flux at the Breaking Line ($t \cdot m/m$)
NE	- 3,450
ENE	- 1,440
E	- 2,020
ESE	- 13,020
SE	+ 63,080
SSE	+ 867,300
S	+ 32,550
Total	+ 943,000

Table 4. Longshore wave energy flux calculated on the basis of waves estimated during 5 years from Jan. 1971 to Dec. 1975

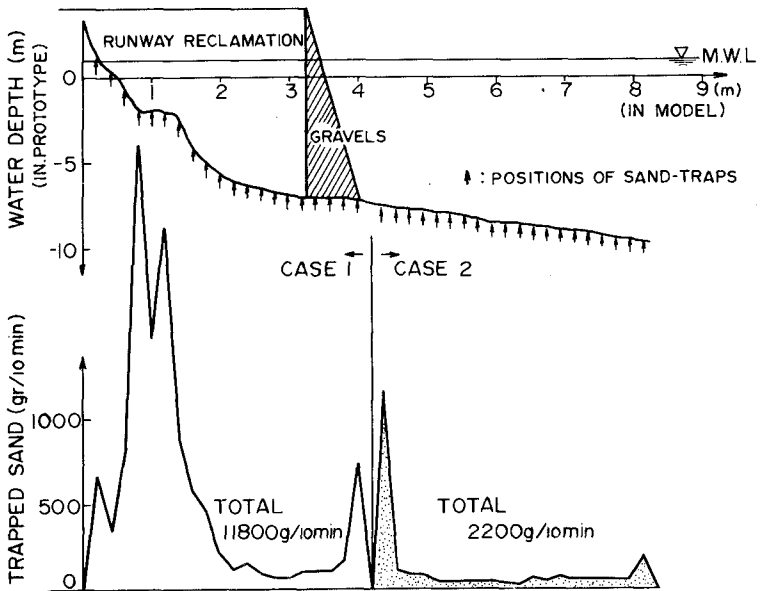


Figure 15. Volume of sand trapped by the sand traps

transport rate is obtained to be $40000 \text{ m}^3/\text{year}$. This value is of the same order as that obtained in the model test. Therefore, the model test would also be considered to be similar to the prototype from the viewpoint of sand transport rate.

CONCLUSIONS

A movable bed model test has been conducted in order to estimate the changes of the bottom topography, mainly in the vicinity of the shoreline, which are caused by a reclamation of 600 m long injected into the sea for the extension of the runway of Tokushima Airport. The Matsushige coast, where the airport is located, is a sandy beach of nearly 4000 m long which is bounded by the breakwater of Imagiri Port to the north and by that of Awazu Port to the south. The model scale is 1/200 horizontal and 1/50 vertical, the sand with median diameter of 0.29 mm was used as movable material. The wave condition for the main test was selected so that the shoreline changes for the past five years from 1964 to 1969 would be reproduced and the quantity of the sand movement in the offshore zone of the model would be similar to that during the normal storm condition in the prototype.

From the main test using the above mentioned wave condition, the following points would be estimated:

(1) The volume of the net longshore sediment transport is about several ten thousands cubic meters per year on the basis of the volume trapped by sand traps, which agrees with the volume calculated from wave energy data

(2) The area where the beach disappears would gradually extend northward, if the coast remains in the present state without any countermeasures.

(3) The reclamation for the runway extension makes the length of the beach which will disappear less than in the case without reclamation.

(4) Double lines of offshore breakwaters are much more effective than a single line of them for restoring the eroded beach in the southern part of the coast.

(5) The area between the runway reclamation and the breakwater of Awazu Port will have a concave shoreline with slight erosion in the center. Offshore breakwaters are useful to prevent this change.

(6) The runway reclamation also decreases the littoral transport entering Awazu Port from the south, after passing the tip of its breakwater.

ACKNOWLEDGEMENTS

The authors express grateful thanks to the members of the Komatsujima Port Construction Office and the Kobe Investigation and Design Office of the 3rd Port and Harbour Construction Bureau, who conducted the field observation for this study, and Mr. Toshihiko Nagai of the same as the authors who engaged in this study.

REFERENCES

- 1) Johnson, J. W. (1949): Scale effects in hydraulic model involving

- wave motion, Trans. Am. Geophys. Union, Vol. 30, No. 4, pp. 517-525
- 2) Iwagaki, Y. and H. Noda (1963): Laboratory study of scale effects in two dimensional beach processes, Proc. 8th Conf. on Coastal Eng., pp. 194-210
 - 3) Sato, S., T. Ijima, and N. Tanaka (1963): A study of critical depth and mode of sand movement using radioactive glass sand, Proc. 8th Conf. on Coastal Eng., pp. 304-323
 - 4) Savage, R. P. (1962): Laboratory determination of littoral transport rate, Proc. Am. Soc. Civil Engrs. No. WW2, pp. 69-92
 - 5) Sato, S. (1963): Study of sand drift phenomena related to new port projects, Tech. Note of The Port and Harbour Research Inst., No. 5 (Japanese)

APPENDIX

Surface Layer Movement and Completely Active Movement of Bottom Sand

Sato-Ijima-Tanaka (1963)³ have classified the distribution patterns by waves of radioactive glass sand injected in the offshore zone into the following four groups shown in Figure A-1:

(1) The first group This is the case that the point of the maximum count moves in the direction of the wave propagation and all equi-count lines also extend in the same direction.

(2) The second group This is the case that the point of the maximum count does not move, but all equi-count lines extend in the same direction of the wave propagation.

(3) The third group This is the case that the point of the maximum count does not move and only a part of equi-count lines extends in the direction of wave propagation. This group also contains the case that the count decreases markedly in total, despite the distribution of equi-count lines scarcely changes.

(4) The fourth group This is the case that the distribution of equi-count lines remains unchanged and the count also does not decrease significantly. The cases that all equi-count lines extend in the same direction as the tidal current or in the direction opposite to the wave propagation are also included in this group.

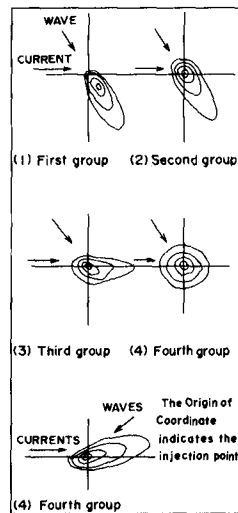


Figure A-1

Then, classifying the field data into these four groups, the results that they have been related with the wave characteristics are shown in Figure A-2⁵. This figure was obtained by Sato (1963)⁵, who plotted additional data in the similar figure by Sato-Ijima-Tanaka (1963)³. In the figure, wave height H and wave period T are those of the maximum significant wave at the injection point of glass sand during the period when the change of count-lines was monitored, and depth h the mean water

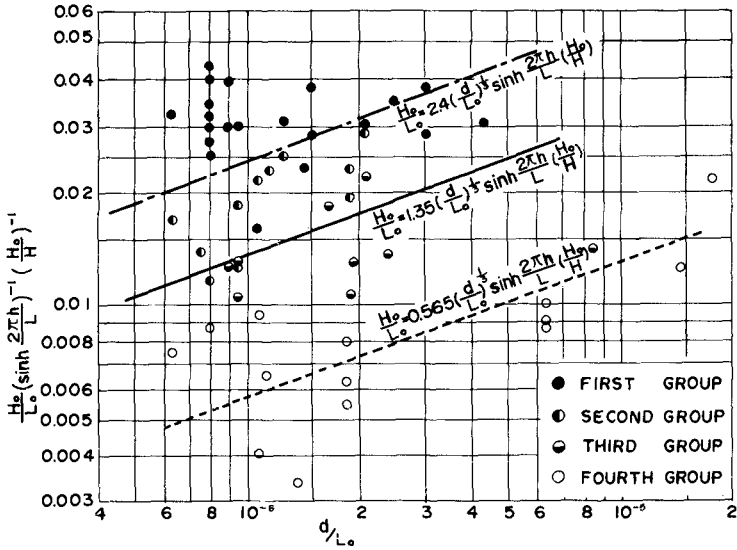


Figure A-2. Relation between the wave characteristics and the median diameter of sand for each distribution of radioactive glass sand (Sato-Ijima-Tanaka 1963 and Sato 1963)

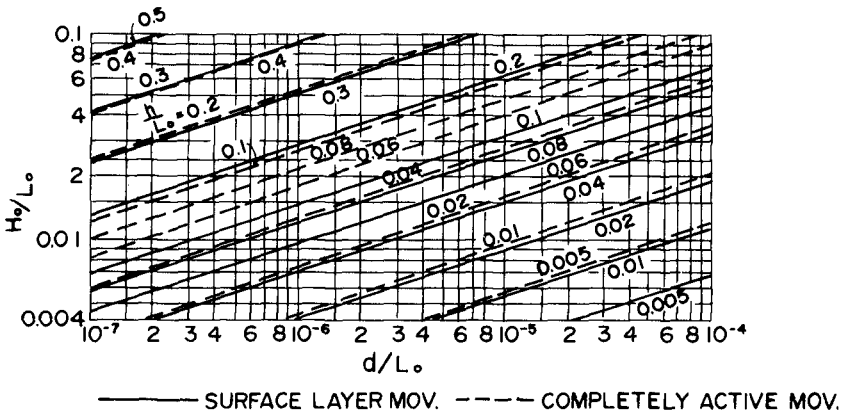


Figure A-3. Calculation diagram of Eqs. (A-1) and (A-2)

depth at the injection point. H_0 and L_0 are the height and length of the deep water wave for H and T , d the median diameter of the glass sand which is the same as the bottom sand in the vicinity. In this figure, the transition from the second group to the third group is shown by the following equation:

$$\frac{H_0}{L_0} = 1.35 \left(\frac{d}{L_0}\right)^{1/3} \sinh \frac{2\pi h}{L} \cdot \left(\frac{H_0}{H}\right) \quad (A-1)$$

and the critical condition on which points enter into the first group is shown by the following equation:

$$\frac{H_0}{L_0} = 2.4 \left(\frac{d}{L_0}\right)^{1/3} \sinh \frac{2\pi h}{L} \cdot \left(\frac{H_0}{H}\right) \quad (A-2)$$

That is, Equation (A-1) corresponds to the state where all sand particles on the surface layer of the sea-bed move collectively in the direction of wave propagation and Equation (A-2) corresponds to such great movement of the bottom sand as to produce the change of water depth. The former is called the surface layer movement and the latter the completely active movement by Sato and Tanaka. Figure A-3 shows the calculation diagrams of those equations.